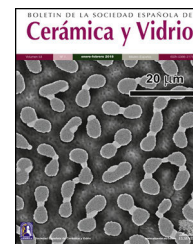




BOLETIN DE LA SOCIEDAD ESPAÑOLA DE  
**Cerámica y Vidrio**

[www.elsevier.es/bsecv](http://www.elsevier.es/bsecv)



## Recycling of residual boron muds into ceramic tiles

Chiara Zanelli<sup>a</sup>, Eduardo Domínguez<sup>b</sup>, Claudio Iglesias<sup>c</sup>, Sonia Conte<sup>a,\*</sup>,  
 Chiara Molinari<sup>a</sup>, Roberto Soldati<sup>a</sup>, Guía Guarini<sup>a</sup>, Michele Dondi<sup>a</sup>

<sup>a</sup> CNR-ISTEC, Istituto di Scienza e Tecnologia dei Materiali Ceramici, Faenza 48018, Italy

<sup>b</sup> Departamento de Geología, Universidad Nacional del Sur, Bahía Blanca 8000, Argentina

<sup>c</sup> Piedra Grande SA, Trelew, Chubut 9100, Argentina

### ARTICLE INFO

#### Article history:

Received 27 July 2018

Accepted 16 January 2019

Available online 21 February 2019

#### Keywords:

Boron sludge

Ceramic flux

Stoneware tiles

Waste recycling

### ABSTRACT

Waste recycling has become an important issue in the environmental sustainability of mining operations. Beneficiation of borate ores produces a boron-bearing sludge, which utilization in ceramic manufacturing may lower the process energy demand. A case-study was carried out on a sludge coming from the processed ore of an evaporite located at the Tincalayu mine in the Salta province, Argentina. The use in vitrified tiles of this sludge was appraised addressing key-points in processing and product performances. The sludge was added to stoneware batches (up to 10% wt.) and tested at the laboratory scale. It consists of feldspars, quartz, illite and chlorite, plus ulexite (6.4% B<sub>2</sub>O<sub>3</sub>) that turns this sludge into a powerful flux. The waste had a minor effect during milling but allowed an improved compaction. The reactivity during firing was increased: the maximum temperature can be reduced from 1200 °C down to 1140 °C, according to the amount of sludge added. Stoneware tiles have a suitable technical performance, but the sludge tends to lower bulk density and increase closed porosity. Although the influence on phase composition is apparently limited, the sludge can significantly change the melt composition (enriched in boron and alkaline-earth oxides) which governs the sintering behavior. The actual amount of boron sludge recyclable in vitrified tiles is up to 5% by weight.

© 2019 SECV. Published by Elsevier España, S.L.U. This is an open access article under the CC BY-NC-ND license (<http://creativecommons.org/licenses/by-nc-nd/4.0/>).

### Reciclado de lodos residuales con contenido de boro en baldosas cerámicas

#### RESUMEN

El reciclaje de desechos se ha convertido en un tema importante en la sostenibilidad ambiental de las operaciones mineras. El beneficio de los minerales de borato produce un lodo que contiene boro, cuya utilización en la fabricación de cerámica puede reducir la demanda de energía del proceso. El lodo estudiado proviene del mineral procesado de una evaporita ubicada en la mina Tincalayu en la provincia de Salta, Argentina. El uso en azulejos vitrificados de ese lodo se evaluó abordando los puntos clave en el procesamiento y el rendimiento del producto. El lodo se agregó a los lotes de gres (hasta el 10% en peso) y se probó a escala de laboratorio. Se compone de feldespatos, cuarzo, illita y clorita, más ulexita (6,4% B<sub>2</sub>O<sub>3</sub>)

#### Palabras clave:

Lodo de boro

Fundente cerámico

Azulejos de gres

Reciclaje de residuos

\* Corresponding author.

E-mail address: [sonia.conte@istec.cnr.it](mailto:sonia.conte@istec.cnr.it) (S. Conte).

<https://doi.org/10.1016/j.bsecv.2019.01.002>

0366-3175/© 2019 SECV. Published by Elsevier España, S.L.U. This is an open access article under the CC BY-NC-ND license (<http://creativecommons.org/licenses/by-nc-nd/4.0/>).

que convierte este lodo en un poderoso fundente. El desecho tuvo un efecto menor durante la molienda, pero permitió una compactación mejorada. La reactividad durante la cocción aumentó: la temperatura máxima se puede reducir de 1200 °C a 1140 °C, según la cantidad de lodo añadida. Las baldosas de gres tienen un rendimiento técnico adecuado, pero el lodo tiende a reducir la densidad aparente y aumentar la porosidad cerrada. Aunque la influencia en la composición de la fase es aparentemente limitada, el lodo puede cambiar significativamente la composición de la masa fundida (enriquecida en óxidos de boro y alcalino-térreos) que rige el comportamiento de sinterización. La cantidad real de lodo reciclable en baldosas vitrificadas es hasta el 5% en peso.

© 2019 SECV. Publicado por Elsevier España, S.L.U. Este es un artículo Open Access bajo la licencia CC BY-NC-ND (<http://creativecommons.org/licenses/by-nc-nd/4.0/>).

## Introduction

During the last two decades, waste recycling turned to be an important issue in the environmental sustainability of mining operations, improving the efficiency in natural resources consumption. This is particularly true in the borate industry, where the ore beneficiation produces boron-bearing residues with a potential as ceramic flux. Argentina is an important boron producer with a yearly output of 170,000 tons of borax and boric acid compounds.

The borate ores residues have been extensively investigated in the latest years [1]. Apart from an early experiment with a processing waste from the Inder borate deposit in Kazakhstan [2], residues came in all cases from beneficiation plants in Turkey [3,4]: mostly from the Kirka-Emet borax deposit [5], and some from the Bigadiç colemanite-ulexite deposit [6] or the Bandırma plant and the Kestelek colemanite deposit [7]. The recycling of boron-containing wastes has been assessed in clay bricks [8–16], ceramic tiles [17–25], as well as ceramic frits and glazes [26–31]. The chemical composition of these boron wastes is summarized in Table 1.

All these studies agree about the technological feasibility of utilizing borate residues, even though with different amounts depending on the end-use. The recommended waste percentages are on average higher in clay bricks (up to 30 wt.%) than in ceramic tiles (up to 8 wt.%) and glazes (up to 5 wt.%). To compare these values properly, the threshold indicated in the literature is expressed as B<sub>2</sub>O<sub>3</sub> weight percent in the final product (Table 2).

According to these figures, clay bricks can tolerate an amount of B<sub>2</sub>O<sub>3</sub> widely spanning from around 1% [11,13,14] to 5–6% [12,16]. In the case of glazes, this percentage seems to be ≤1% [28,29]. The optimal amount of B<sub>2</sub>O<sub>3</sub> tolerable in tile bodies fluctuates from 0.1% to 1.3%, even so it is apparently lower for porous products (wall tiles) than for vitrified tiles (porcelain stoneware). However, while for porous tiles there are several data ranging from ≤0.5 B<sub>2</sub>O<sub>3</sub> [20,21,25] to approximately 1% B<sub>2</sub>O<sub>3</sub> [17,19], only one figure (1.3% B<sub>2</sub>O<sub>3</sub>) exists for porcelain stoneware tiles [23]. This range matches the results of experiments carried out on bodies containing different borate fluxes: borax [2,32–34], boric acid [33,34], tincalconite [33–35], colemanite [36,37], ulexite [37–39], hydroboracite [32,37], datolite [2], and borosilicate frit [40], which effect in tile batches has been widely investigated (Table 2).

The present study is aimed at appraising the use of the boron sludge coming from the Tincalayu mine (Argentina) into stoneware tile batches, addressing key-points in processing and product performance. The rationale consists in adding increasing waste amounts (up to 10 wt.%) then testing their technological behavior at the laboratory scale and finally characterizing semi-finished and finished products in order to assess the technological feasibility.

## Experimental

The boron sludge comes from the processed ore of the Tincalayu mine, located at the western end of the Salar del Hombre Muerto in the Salta province, Argentina (67°03' W and 25°16' S, Fig. 1) at an elevation of 3700–4000 m above the mean sea level [41].

The Tincalayu mineralization occurs in a fractured, folded and elevated block, at the middle third of the Upper Miocene Sijes Formation that lies over the Ordovician metamorphic basement and is covered by Pleistocene conglomerates [42]. The ore layer extends over a 0.15 km<sup>2</sup> area with an average thickness of 40 m. Genetically, it is an evaporite with a complex evolution. Although it is almost monomineralic in composition, with crystals or masses of borax as the major component, at least 16 boron species were recognized in the deposit [43].

An expansion of the Tincalayu operation from its current 30,000 ton/year production to 120,000 ton/year is under way.

The sludge sample is a mixing product of several aliquots taken during a routine industrial processing day at the concentration plant (Campo Quijano, Salta). It stems from the borax production after a hot water ore leaching (180 °C). The resulting solution is subsequently decanted and filtrated to separate the sludge that is discarded as a waste. This sludge, previously dried, was characterized by:

- chemical analysis (major oxides and minor elements by Inductively-Coupled Plasma Mass Spectroscopy, ICP-MS);
- mineralogical composition by X-ray powder diffraction (XRPD, D8 Advance equipped with LynxEye detector, Bruker, Germany);
- test fusibility by hot-stage microscopy (Misura 3, Expert System Solutions, Italy) with heating rate 10 °C min<sup>-1</sup> until melting.

**Table 1 – Chemical composition of residues from beneficiation of boron ores investigated in literature in comparison of the Tincalayu boron sludge.**

wt. %	Tincalayu sludge (this work)	Borax												Colemanite			Szajbélyte
		[9]	[10]	[10]	[11]	[12]	[13]	[14]	[16]	[19]	[20]	[24]	[25]	[8]	[22]	[31]	[2]
SiO <sub>2</sub>	50.48	18.74	8.26	12.53	17.31	19.97	15.10	19.64	13.47	17.10	15.83	23.03	15.55	16.67	29.05	16.10	40.00
TiO <sub>2</sub>	0.43	–	–	–	–	0.05	–	–	–	0.03	0.01	0.25	–	–	0.03	–	–
B <sub>2</sub> O <sub>3</sub>	6.36	8.15	11.92	13.09	5.87	14.30	12.60	20.12	16.31	11.00	3.99	21.25	8.02	14.09	9.61	19.67	2.80
Al <sub>2</sub> O <sub>3</sub>	11.67	3.24	0.09	0.44	0.34	2.44	1.70	0.77	1.02	2.60	1.06	7.22	1.52	0.94	2.63	0.89	2.30
Fe <sub>2</sub> O <sub>3</sub>	3.13	0.47	0.13	0.24	0.33	0.50	0.20	0.28	0.25	0.40	0.24	3.11	0.42	0.35	0.26	0.11	3.00
MgO	4.65	16.63	15.56	14.97	17.97	13.75	14.20	9.51	12.60	15.40	19.84	7.37	18.31	11.8	14.57	6.91	0.50
CaO	4.30	21.85	10.75	11.18	17.55	11.37	16.80	8.29	12.01	16.90	20.66	14.98	17.80	13.53	17.16	26.41	33.50
SrO	–	–	1.23	0.67	1.30	1.06	–	–	–	–	–	–	1.09	–	–	1.23	–
Na <sub>2</sub> O	5.56	6.83	7.63	8.67	2.86	7.50	4.10	12.20	7.43	2.90	2.58	0.06	5.32	6.87	1.02	0.22	–
K <sub>2</sub> O	2.12	0.33	–	–	5.05	2.34	0.60	0.66	–	1.10	0.63	2.10	0.72	–	0.12	0.51	0.10
L.o.I.	11.30	22.83	43.33	36.24	31.42	26.72	34.10	28.53	24.30	28.90	35.16	20.98	30.76	35.75	25.20	27.98	17.89
Total	100.00	99.07	98.90	98.03	100.00	100.00	99.40	100.00	87.39	96.33	100.00	100.35	99.51	100.00	99.65	100.03	100.09

**Table 2 – Utilization in the ceramic production of residues from the beneficiation of borate ores and borate industrial minerals. Recommended amount and corresponding B<sub>2</sub>O<sub>3</sub> concentration in the finished product.**

Ceramic product	Maximum amount of waste recommended (wt.%)	Corresponding to B <sub>2</sub> O <sub>3</sub> wt.% (dry basis)	Reference
Clay brick	10	2.2	[8]
Clay brick	30	3.2	[9]
Clay brick	15	3.2	[10]
Clay brick	10	0.9	[11]
Clay brick	30	5.9	[12]
Clay brick	5	1.0	[13]
Clay brick	3	0.8	[14]
Clay brick	2	?	[15]
Clay brick	20	5.2	[16]
Ceramic tile (?)	3	2.0	[2]
Ceramic tile	4	1.1	[17]
Ceramic tile	6	1.0	[19]
Ceramic tile	8	0.5	[20]
Ceramic tile	2	0.1	[21]
Ceramic tile	5	0.6	[22]
Ceramic tile	5	1.3	[23]
Ceramic tile	1.4	0.2	[25]
Glaze	2	0.4	[28]
Glaze	5	1.0	[29]
Borate industrial mineral	Borate successfully added to the ceramic body (wt.%)	Corresponding to B <sub>2</sub> O <sub>3</sub> wt.% (dry basis)	Reference
Borax	0.9	0.62	[32]
Borax	1.0	0.69	[33]
Borax	0.4	0.28	[34]
Boric acid	1.0	1.00	[33]
Boric acid	0.4	0.40	[34]
Borosilicate frit	4.0	3.52	[40]
Colemanite	2.5	1.23	[37]
Datolite	5.0	0.83	[2]
Hydroboracite	0.9	0.62	[32]
Hydroboracite	2.5	1.40	[37]
Tincalconite	1.0	0.69	[33]
Tincalconite	0.4	0.28	[34]
Tincalconite	3.0	2.17	[35]
Ulexite	2.5	1.43	[37]
Ulexite	0.5	0.33	[38]
Ulexite	0.5	0.33	[39]

The boron waste behavior was tested into stoneware batches (2-5-10 wt.%) and compared with reference bodies. The batches were designed by two different strategies: adding boron waste in replacement of ball clay (“Argentinian-style bodies” A0 to A10) and in substitution of Na-feldspar (“Italian style bodies” B0 to B10) (Table 3). The changes in the bulk chemical composition of the batches due to replacement of Na-feldspar or ball clay by the boron waste are shown in Table 3. In any case, the introduction of boron sludge induced a slight decrease in SiO<sub>2</sub> and Al<sub>2</sub>O<sub>3</sub> together with a slight increase of CaO, MgO, K<sub>2</sub>O and loss ignition. The Na<sub>2</sub>O amount tends to decrease in the “Italian-style” bodies but to increase in the “Argentinian-style” ones.

Simulation of the industrial tile making processing was carried out at the laboratory scale by wet milling (15 min in planetary mill with porcelain jar and alumina grinding media). The slip so obtained (~60% solid load, 0.3% Na-tripolyphosphate) was oven dried and de-agglomerated (hammer mill with grid of 500 μm) prior manual granulation (sieve 2 mm, powder moisture ~8 wt.%). Powders were shaped

into disks (50 mm diameter × 5 mm thickness) by hydraulic pressing (40 MPa) then dried in oven (105 °C overnight) and fast fired in electric kiln (51 min cold-to-cold at max temperature from 1120 to 1240 °C). Data interpretation allowed to get two key indicators: (i) the temperature of maximum densification (T<sub>md</sub>) as indicated by the maximum value of bulk density; (ii) the maturing temperature (T<sub>BI</sub>), i.e. the temperature corresponding to 3% of water absorption (prescribed as threshold for BI stoneware tiles by standard ISO 13006) in the sintering curve.

The technological properties were measured on both semifinished and finished products. The particle size distribution was determined on milled bodies by X-ray monitoring of gravity sedimentation (SediGraph 5100, Micromeritics, UK). Green and dry samples were tested for working moisture (ASTM C324), springback (i.e., 100\*(D<sub>p</sub> - D<sub>m</sub>)/D<sub>m</sub>, where D<sub>p</sub> is the diameter of the pressed disk and D<sub>m</sub> is the diameter of the mold), drying shrinkage (ASTM C326) as well as green and dry bulk density (weight-to-volume ratio). The following technological properties were determined on fired samples:

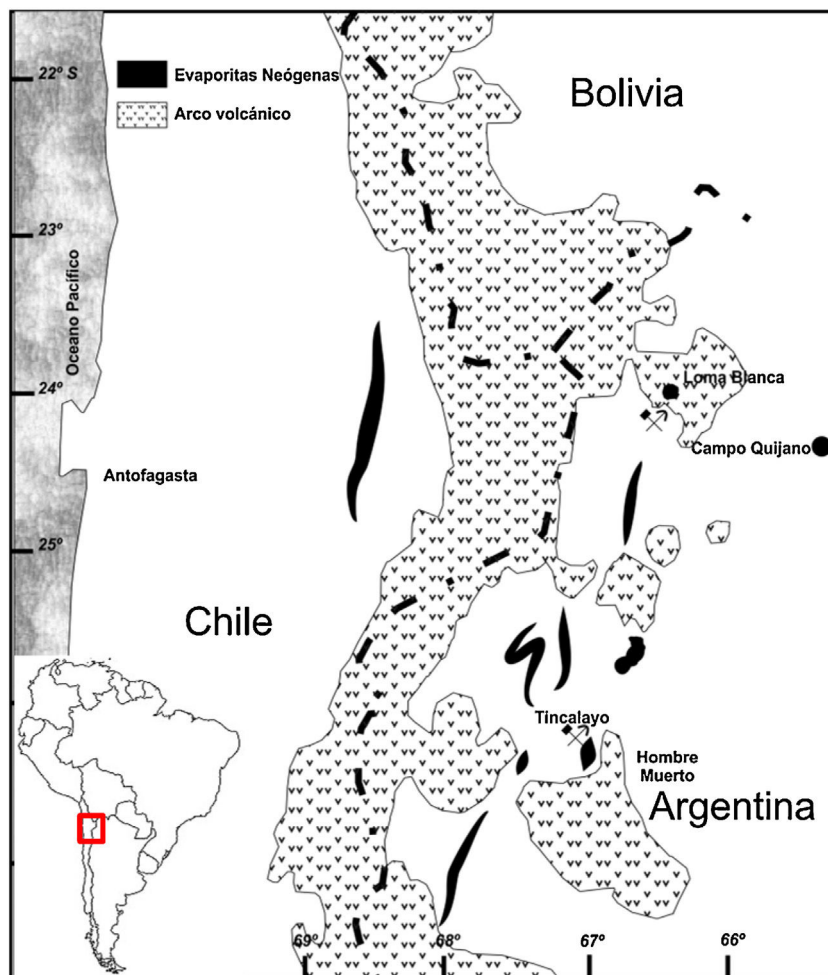


Fig. 1 - Location of the boron deposit, Tincalayu, Salta, Argentina.

Table 3 - Raw materials and chemical composition of stoneware batches.

Ingredients (wt%)	A0	A2	A5	A10	B0	B2	B5	B10
Ball clay 1	30	28	25	20	25	25	25	25
Ball clay 2	15	15	15	15	15	15	15	15
Pyrophyllitic clay	20	20	20	20	-	-	-	-
Na-feldspar	-	-	-	-	20	18	15	10
Na-K feldspar	35	35	35	35	12.5	12.5	12.5	12.5
K-Na feldspar	-	-	-	-	12.5	12.5	12.5	12.5
Quartz sand	-	-	-	-	15	15	15	15
Boron waste	0	2	5	10	0	2	5	10
SiO <sub>2</sub>	66.9	66.5	65.9	64.9	69.7	69.3	68.8	67.8
TiO <sub>2</sub>	0.3	0.3	0.3	0.3	0.5	0.5	0.6	0.6
B <sub>2</sub> O <sub>3</sub>	-	0.1	0.3	0.6	-	0.1	0.3	0.6
Al <sub>2</sub> O <sub>3</sub>	21.3	21.2	21	20.6	18.1	18	17.8	17.5
Fe <sub>2</sub> O <sub>3</sub> total	0.7	0.7	0.8	0.9	0.7	0.8	0.9	1
MgO	0.2	0.3	0.4	0.6	0.4	0.5	0.6	0.8
CaO	0.3	0.4	0.5	0.7	0.9	1	1.1	1.3
Na <sub>2</sub> O	1.8	1.9	2.1	2.4	3.3	3.2	3.1	2.9
K <sub>2</sub> O	3	3.1	3.1	3.2	2.6	2.7	2.7	2.8
L.o.I.	5.5	5.6	5.6	5.8	3.6	3.8	4.1	4.7

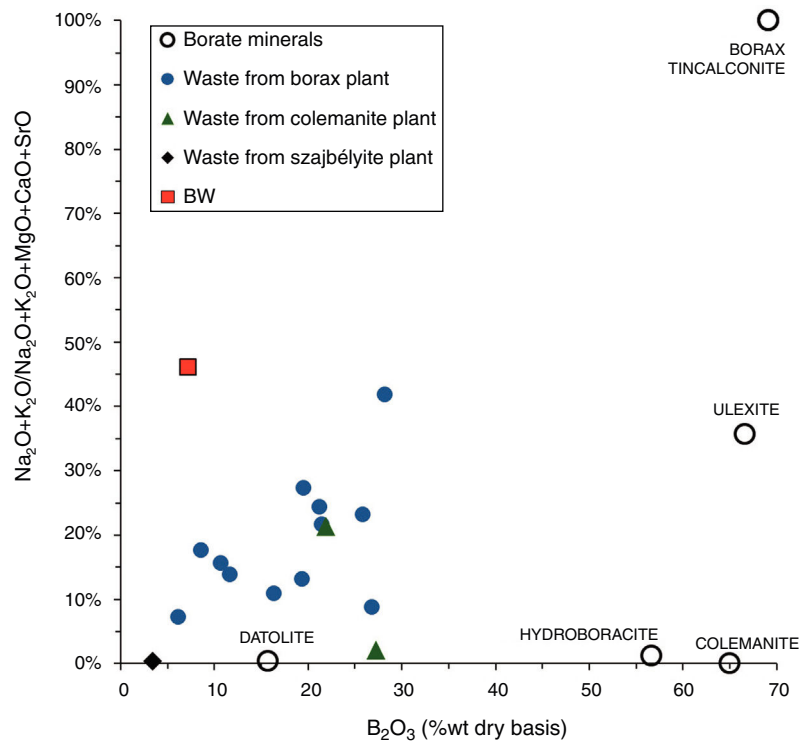


Fig. 2 – Chemical composition of borate wastes and ores proposed as raw materials for ceramics.

linear shrinkage (i.e.,  $100(D_m - D_f)/D_m$  where  $D_f$  is the diameter of the fired disk and  $D_m$  is the diameter of the mold), water absorption, open porosity and bulk density (ISO 10545-3).

The phase composition was quantitatively assessed on samples fired at  $T_{md}$  by X-ray powder diffraction (XRPD, D8 Advance equipped with LynxEye detector, Bruker, Germany). A full profile interpretation by Rietveld refinement was carried out with the GSAS-EXPGUI software package [44,45]. The samples were admixed with 20 wt.% of  $Al_2O_3$  as internal standard to determine the vitreous phase by difference, i.e., 100% minus the sum of crystalline phases [46–48]. The chemical composition of mullite was inferred from the unit cell parameter  $a$ , according to the method of Ban and Okada [49]. The chemical composition of the vitreous phase was calculated on the basis of the bulk chemistry and phase composition. Viscosity and surface tension of the glassy phase at  $T_{md}$  were calculated from its chemical composition, using models developed for glasses and silicate melts [50–52].

## Results and discussion

### Main properties of Tincalayu boron sludge

The Tincalayu sludge is characterized, from the chemical point of view, by peculiar features: its amount of boron oxide (about 6%) is associated to the highest percentages of silica and alumina among borate wastes investigated in the literature (Table 1). On the other hand, alkaline-earth oxides and the loss on ignition are lower than values of wastes from Turkey [8–31], while alkalis fall within the overall variability. This can be clearly appreciated by comparing the boron amount versus the

alkaline-to-alkaline earth oxides ratio (Fig. 2) of borate wastes and typical borate minerals used in ceramic production (i.e. ulexite, colemanite, hydroboracite, etc.). These features are undoubtedly an advantage for the utilization of the Tincalayu waste in vitrified tiles. However, iron oxide is higher than that usually found in Turkish wastes: this circumstance can be considered a limitation for application in white-firing bodies. The high amounts of boron, alkalis and alkaline-earths in the Tincalayu sludge induce a strong fusibility, witnessed by a melting temperature close to  $1100^\circ C$  (Fig. 3A). This value is almost  $300^\circ C$  lower than a strong ceramic flux (nepheline syenite) and nearly  $600^\circ C$  below typical fluxes used in stoneware tiles, like granite and arkosic sands [53,54]. It can be estimated that the addition of boron waste sludge to a standard feldspathic flux determines a lowering of the sintering temperature from  $1240^\circ C$  (boron-free) to  $980^\circ C$  with 10% waste (Fig. 3B).

The mineralogical composition of the Tincalayu boron sludge is characterized by ~45 wt.% plagioclase, ~20 wt.% quartz, ~20 wt.% illite-muscovite, ~10 wt.% ulexite and ~5 wt.% clinochore (Fig. 4). These peculiar treats make it a strong flux able to affect not only the sintering kinetics, but perhaps to change the reactions path during the firing process.

### Technological behavior of unfired bodies

The addition of boron waste sludge does not modify significantly the technological behavior of stoneware tiles during milling, shaping and drying; the main alterations appear to be tolerable in the industrial practice. In general, the waste sludge addition had the following effects:

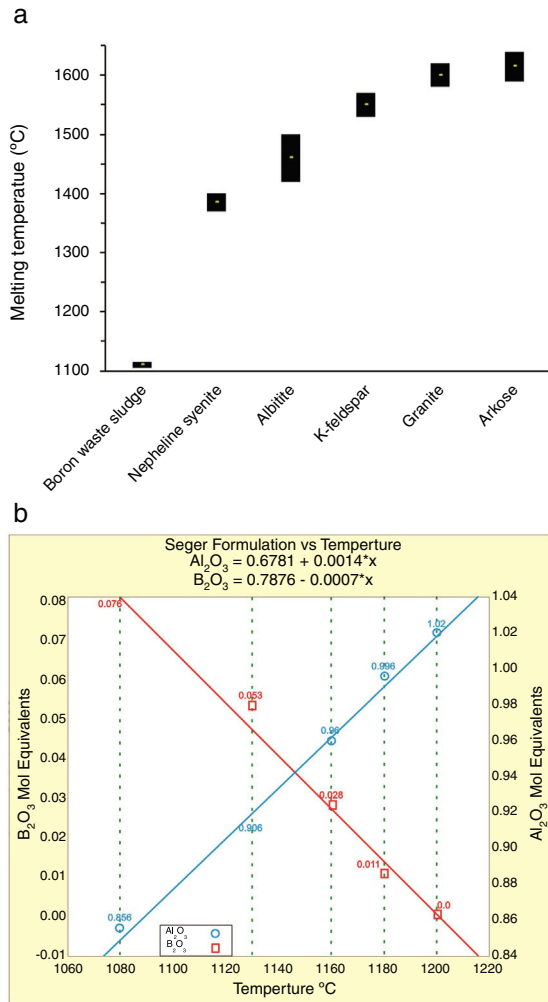


**Fig. 3 – Fusibility chart of the boron waste sludge in correlation with ceramic fluxes [53,54]. Melting behavior of boron waste sludge: hot-stage microscope melting point compared with ceramic flux (a); effect of boron waste additions to a standard feldspathic flux in terms of sintering temperature (b) 0.22 and 0.41 are the Seger equivalent to 5% and 10% boron waste addition.**

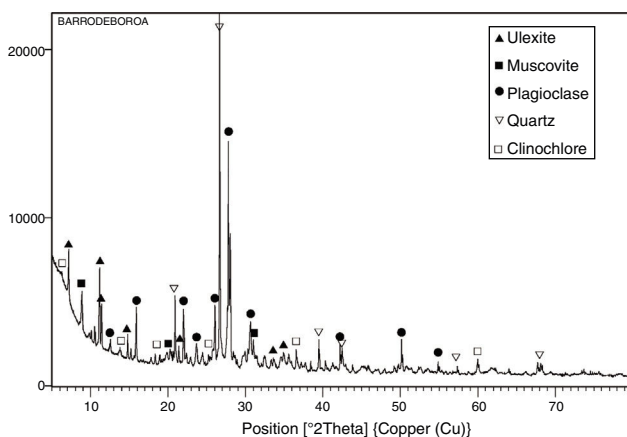


**Fig. 4 – X-ray pattern of the Tincalayu boron sludge.**

- the particle size distribution of waste-bearing slips turned gradually finer, implying a better grindability with respect to feldspathic materials that sludges had replaced (Fig. 5a);
- a slight reduction of the powder moisture required for pressing in both series (Fig. 5b);
- the springback keeps in the range usually accepted in the industrial practice, i.e. 0.3–0.6 cm/m (Fig. 5c);
- the compaction is improved, as the bulk density of dry bodies increased with the boron waste additions (Fig. 5d).

### Technological behavior of fired bodies

The boron waste sludge has distinct effects on firing behavior in the two series of batches (Fig. 6). In the Argentinian-style bodies, the firing shrinkage increases with the amount of boron waste. In addition, the sintering kinetics is improved, as the body with 10% waste (A10) exhibits the larger shrinkage (~6%) already after firing at 1160 °C. The limited shift of  $T_{md}$  to lower temperatures, from 1240 °C of the reference body to 1200 °C of the body A10, is contrasted by a marked effect on the water absorption curves. In fact, the  $T_{BI}$  goes down from 1220 °C of the waste-free body to 1190 °C (A2), 1155 °C (A5) and below 1150 °C for A10.

In the Italian-style batches, a clear reduction of  $T_{md}$  is observed while increasing the waste addition: from 1200 °C of the boron-free body to 1140 °C for the body with 10% of waste (B10). At the same time, a conspicuous shift of the water absorption curves toward lower temperatures is observed, with  $T_{BI}$  moving from 1200 °C for both B0 and B2 to 1190 °C for B5 down to 1155 °C for B10 (Fig. 6).

In general, the bulk density increases with boron waste additions in both series, even though the Argentinian-style batches are characterized by a higher density with respect to the Italian-style ones. In any case, the addition of boron-bearing materials determined a peculiar behavior in stoneware bodies, as already observed in the literature [37], which is in contrast with the expected trend in vitrified tiles, where the  $T_{BI}$  requirement is attained when the body is beyond the  $T_{md}$  [55]. Thus, an inversion occurs in the firing shrinkage curve, due to increasing closed porosity, leading to lower values of bulk density. The reason cannot be ascribed to a lower green bulk density [55] but to the improved fusibility ensured by the boron waste.

### Phase composition and microstructure of fired bodies

The phase composition of the bodies fired at  $T_{md}$  is characterized by an amount of vitreous phase in between 51% and 64%: not so high, if compared with typical values of porcelain stoneware [44]. The quantities of the other components (mullite, quartz, feldspars) vary upon the series (Table 4).

Feldspars are completely melted in the Argentinian-style bodies, while a residual plagioclase persists (7–12%) in the Italian-style ones. Quartz tends to a slight decrease in the Argentinian-style bodies, passing from about 24–25% to 18–22% along with the progressive addition of waste. In contrast, quartz values are constant in the B-series.

The percentage of mullite decreases irregularly by increasing the waste addition in both series, with values typical for the Italian-style bodies (5–9%) but a peculiar, very high range

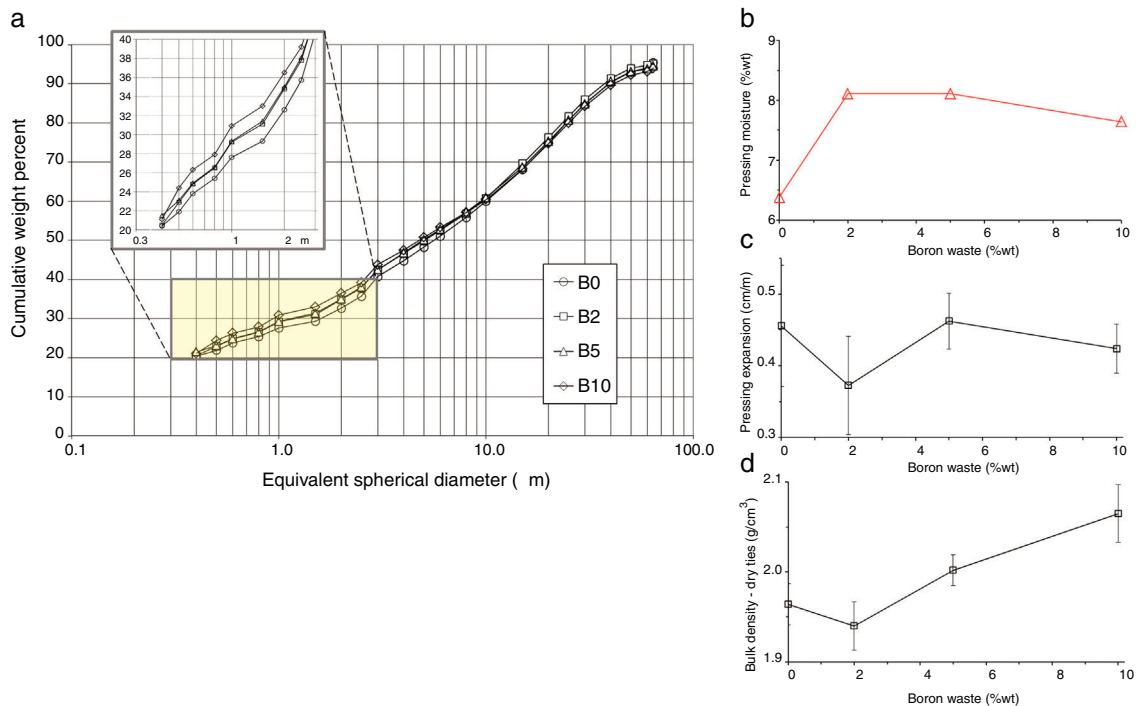


Fig. 5 – Technological behavior of unfired stoneware bodies in function of the amount of waste added: (a) particle size distribution of slips after milling; (b) pressing moisture; (c) springback; (d) dry bulk density.

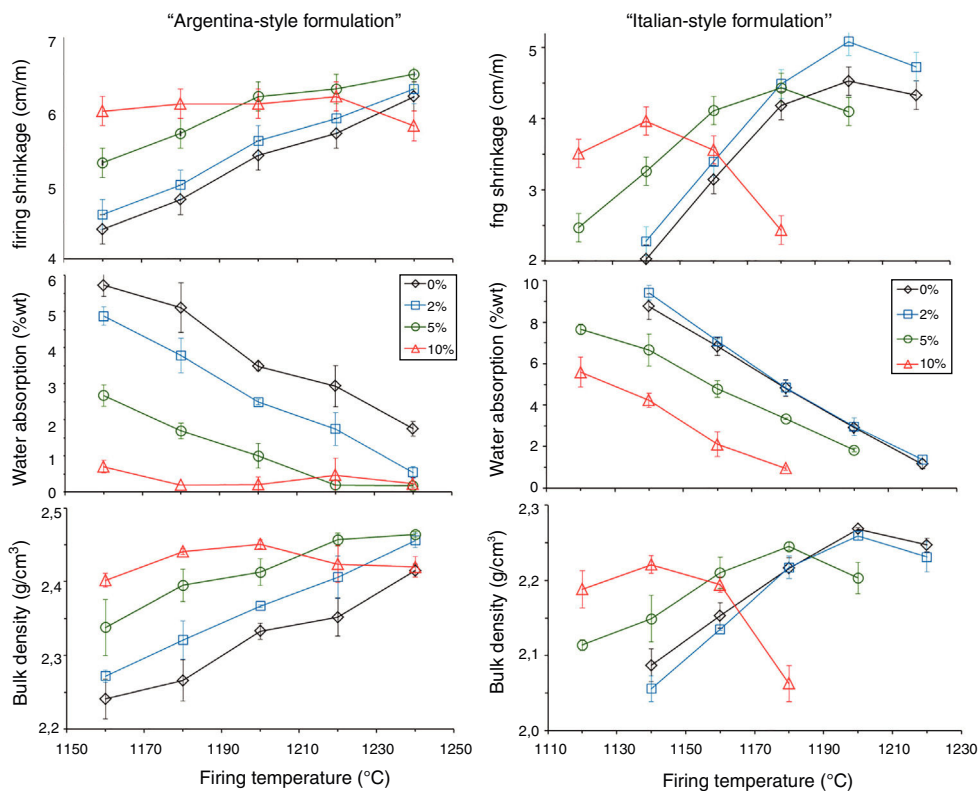


Fig. 6 – Technological properties in function of the firing temperature of stoneware bodies (Argentinian-style on the left and Italian-style on the right).



**Table 4 – Phase composition of the stoneware bodies fired at the temperature of maximum densification ( $T_{md}$ ) and goodness-of-fit ( $RF^2$ ) of Rietveld refinement of XRD patterns.**

Phase	Unit	A0	A2	A5	A10	B0	B2	B5	B10	std.dev.
$T_{md}$	°C	1240	1240	1240	1220	1220	1220	1200	1140	–
Quartz	wt. %	24	25	18	22	25	26	26	25	0.2
Mullite	wt. %	25	21	24	14	7	9	8	5	0.1
Plagioclase	wt. %	–	–	–	–	10	7	12	12	0.1
Vitreous phase	wt. %	51	54	58	64	58	58	54	58	0.4
$RF^2$	1	8.1	9.0	8.0	9.1	8.0	8.9	9.1	9.1	–

in the A-series (14–25%). Mullite exhibits unit cell parameters (particularly the  $a$ -axis length between 7.5398 and 7.5501 Å) corresponding to alumina contents around 60.73 mol%, thus slightly exceeding the  $Al_2O_3:SiO_2 = 3:2$  stoichiometry [49].

The above described fluctuations in the crystalline phases are reflected by the amount of vitreous phase, which increases with the boron waste percent in the Argentinian-style bodies and remains substantially unchanged in the case of Italian-style ones.

The microstructure of stoneware is compact and characterized by a conchoidal fracture, coherently with the rather high amount of glassy phase (Fig. 7). Similar microstructural features occur in both boron-free and boron-bearing bodies, like a few spherical pores (10 to 30  $\mu$ m in diameter).

#### Composition and physical properties of the liquid phase

The chemical composition of the vitreous phase and its physical properties at high temperature are summarized in Table 5.

The different behavior of the two series can be explained by the chemical composition of the liquid phase, which affects the melt viscosity and surface tension, hence the sintering rate.

In particular, the glassy phase becomes poorer in  $SiO_2$ , when the boron sludge is added, mirrored by a decreasing silica saturation index (and conversely an increasing  $B_2O_3/GNF$  ratio, i.e. the fraction of boron oxide over the total amount of glass network formers). The liquid phase of the Argentinian-style bodies turns also richer in  $Al_2O_3$  (with higher alumina saturation index). On the other hand, glass network modifiers (GNM), as well as the share of MgO and CaO over GNM, increase with the sludge addition, but the  $Na_2O/K_2O$  ratio has opposite trends in the A-series (increasing) and in the B-series (decreasing). Iron oxide is growing with the sludge addition in both series.

These compositional changes of the vitreous phase reflect into slightly different values of shear viscosity and surface tension calculated at  $T_{md}$ . In order to let the effect of glass

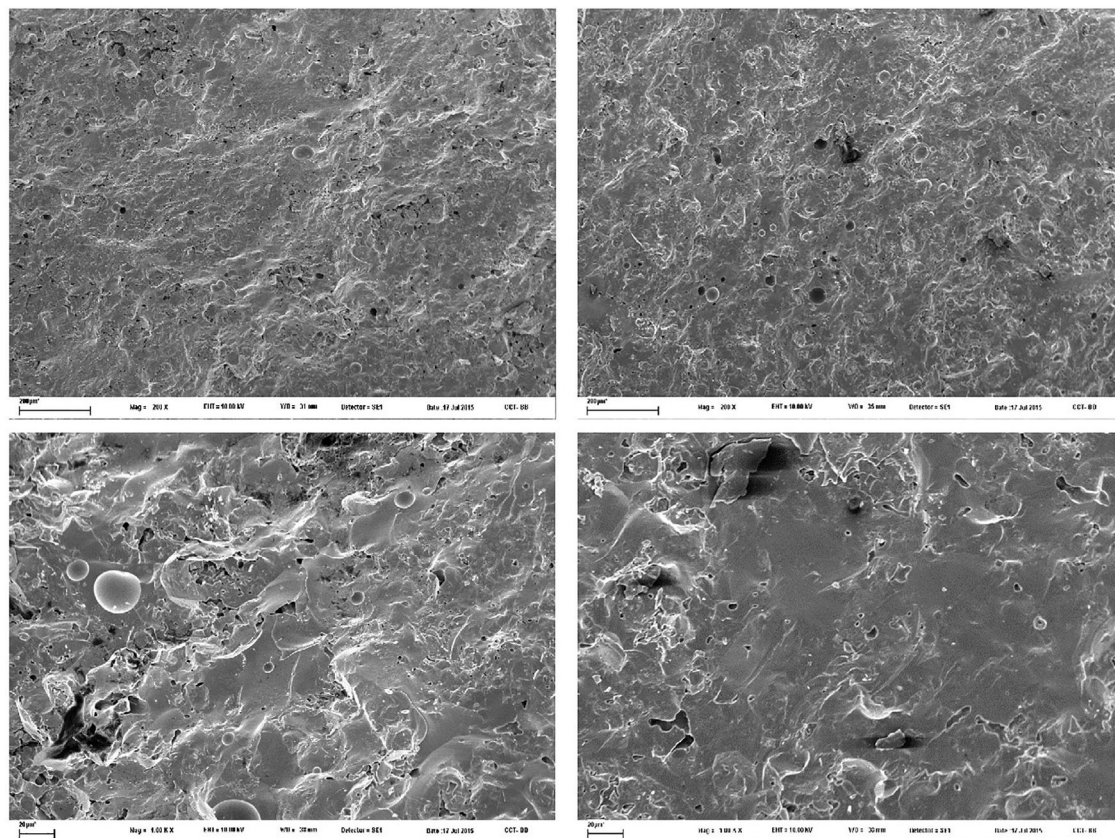


**Fig. 7 – Microstructure of the surface fracture of Italian-style bodies: B0 (left) and B5 (right).**

**Table 5 – Chemical composition and physical properties of the vitreous phase present in the stoneware bodies fired at  $T_{md}$ .**

Phase	Unit	A0	A2	A5	A10	B0	B2	B5	B10	std.dev.
$T_{md}$	°C	1240	1240	1240	1220	1220	1220	1200	1140	–
SiO <sub>2</sub>	wt. %	77.85	73.07	77.67	67.08	66.47	66.90	65.32	62.91	0.20
TiO <sub>2</sub>	wt. %t	0.70	0.67	0.62	0.56	0.96	0.98	1.07	1.03	0.05
B <sub>2</sub> O <sub>3</sub>	wt. %t	0.00	0.25	0.58	1.06	0.00	0.23	0.62	1.15	0.10
Al <sub>2</sub> O <sub>3</sub>	wt. %t	9.08	13.62	8.59	18.43	20.37	18.74	19.42	21.41	0.20
Fe <sub>2</sub> O <sub>3</sub>	wt. %	1.36	1.37	1.41	1.47	1.27	1.38	1.67	1.84	0.05
MgO	wt. %	0.38	0.53	0.74	1.04	0.71	0.87	1.20	1.54	0.05
CaO	wt. %	0.58	0.71	0.89	1.15	1.68	1.81	2.14	2.31	0.05
Na <sub>2</sub> O	wt. %	3.73	3.74	3.79	3.90	3.84	4.31	3.31	2.74	0.10
K <sub>2</sub> O	wt. %	6.32	6.04	5.71	5.31	4.71	4.78	5.25	5.07	0.10
Na <sub>2</sub> O/K <sub>2</sub> O	Molar ratio	0.90	0.94	1.01	1.12	1.24	1.37	0.96	0.82	–
B <sub>2</sub> O <sub>3</sub> /GNF	Molar ratio	0.00	0.30	0.64	1.35	0.00	0.29	0.81	1.56	–
Mg+Ca/GNM	Molar ratio	0.13	0.17	0.22	0.28	0.30	0.31	0.38	0.45	–
G. N. Formers	mole %	83.12	79.70	82.98	75.20	74.03	74.18	73.09	71.45	–
G. N. Modifiers	mole %	9.43	9.82	9.95	11.01	10.66	11.57	11.82	11.92	–
G. N. Intermediates	mole %	7.44	10.48	7.07	13.78	15.31	14.25	15.08	16.63	–
SSI	Molar ratio	32.2	28.2	32.6	22.2	23.9	20.3	21.7	22.7	–
ASI	Molar ratio	0.65	0.97	0.61	1.29	1.41	1.21	1.29	1.51	–
Shear viscosity at $T_{md}$	log <sub>10</sub> Pa s	5.32	5.30	5.20	5.20	5.48	5.18	5.22	5.66	0.02
Surface tension at $T_{md}$	mN m <sup>-1</sup>	349.7	346.6	353.1	362.0	293.6	305.3	311.7	316.4	0.3
Shear viscosity 1220 °C	log <sub>10</sub> Pa s	5.44	5.41	5.32	5.20	5.48	5.18	5.09	5.09	0.02
Surface tension 1220 °C	mN m <sup>-1</sup>	306.9	317.2	307.7	329.8	338.1	334.6	336.6	341.9	0.3
ST/SV at $T_{md}$	mm s <sup>-1</sup>	1.44	1.58	1.92	2.07	1.12	2.20	2.03	0.78	0.02
ST/SV at 1220 °C	mm s <sup>-1</sup>	1.12	1.21	1.48	2.05	1.11	2.18	2.69	2.77	0.3

GNF: Glass Network Formers (SiO<sub>2</sub>+B<sub>2</sub>O<sub>3</sub>). GNM: Glass Network Modifiers (MgO+CaO+Na<sub>2</sub>O+K<sub>2</sub>O). GNI: Glass Network Intermediates (TiO<sub>2</sub>+Al<sub>2</sub>O<sub>3</sub>+Fe<sub>2</sub>O<sub>3</sub>). Mg+Ca/GNM: (MgO+CaO)/(MgO+CaO+Na<sub>2</sub>O+K<sub>2</sub>O). SSI: Silica Saturation Index, i.e. SiO<sub>2</sub>-MgO-(2°CaO)-(6°Na<sub>2</sub>O)-(6°K<sub>2</sub>O). ASI: Alumina Saturation Index, i.e. Al<sub>2</sub>O<sub>3</sub>/(CaO+Na<sub>2</sub>O+K<sub>2</sub>O). ST/SV: ratio of surface tension to shear viscosity.

composition on the physical properties easily appreciable, data are compared also for the same firing temperature (Table 5). While the decrease of glass network formers and the concomitant increase of modifiers induced a gradual reduction of shear viscosity, values of surface tension fluctuate without a clear trend. The variation of network formers ratio is able to explain the viscosity drop, mainly for the well-known fluxing effect of boron [56].

#### Boron effect on firing behavior of stoneware tiles

The occurrence of boron in the liquid phase (together with the further chemical changes induced by the growing addition of sludge) is able to affect significantly the firing behavior. In particular, it is expected to increase the glass-vapor surface tension and, at the same time, to decrease the shear viscosity, once bodies are compared at the same temperature (e.g., 1220 °C in Table 5). These trends should be considered in the light of the viscous flow sintering, which initial rate is predicted to follow the Frenkel's equation [57]:

$$\frac{\Delta L}{L_0} = \frac{3\gamma}{8\eta(T)r} t$$

where  $L_0$  is the starting length of sample,  $\Delta L$  the linear shrinkage after a sintering time  $t$ ,  $\eta(T)$  is the temperature dependent shear viscosity,  $\gamma$  is the glass-vapor surface tension and  $r$  is the starting particle radius. Therefore, the surface tension to shear viscosity ratio (ST/SV) is the most important factor

to determine the sintering rate. Such a ratio is increasing as a consequence of the growing addition of sludge in both series.

However, the strong influence of B<sub>2</sub>O<sub>3</sub> on the fusibility makes it possible to lower the  $T_{md}$ , as already seen in the previous section. Comparing the ST/SV ratio, as estimated at the  $T_{md}$ , two different tendencies arose. An increasing trend can be appreciated for the A-series: it corresponds to the sintering curves, which clearly scale in function of boron content (Fig. 6). For the B-series, which  $T_{md}$  varies widely from 1140 °C to 1240 °C, the trend is not linear and the ST/SV ratio peaks for a content of 2% B<sub>2</sub>O<sub>3</sub> in the finished product.

#### Conclusions

Sludges coming from the beneficiation of borate ores have a great potential as ceramic fluxes, as demonstrated by the case-study of the Tincalayu mine waste and further examples in the literature. Nevertheless, the actual amount recyclable in vitrified tiles has to be defined case by case, due to the wide variability of chemical and mineralogical composition of boron-bearing sludges.

In general, boron plays a powerful fluxing effect in stoneware bodies, which implies both advantages (lower water absorption and open porosity; lower temperature and/or shorter time in firing schedules) and drawbacks (small fluctuation in B<sub>2</sub>O<sub>3</sub> percentage may turn into appreciable changes of technological behavior; lower bulk density due to some closed porosity). However, borates are minor components of

these sludges, which usually consist of a complex mixture of clay minerals, feldspars, and quartz. Thus, their actual behavior during ceramic processing depends on additional factors beyond the boron content (e.g., amount and type of clay minerals).

Although the addition of boron-bearing sludge to stoneware batches is fully tolerable, in technological terms, up to 5% by weight (as shown by the Tincalayu waste) some problem may arise in the industrial practice. In fact, the sludge requires, in force of its strong fluxing effect, an accurate dosage to keep the firing behavior under strict control. A viable route can be envisaged by addressing the waste recycling through the supply chain of conventional fluxes, for instance by incorporating the sludge into feldspathic rocks. This solution is attracting especially in case of quartz-feldspathic raw materials (like granite, rhyolite or arkose) that usually have a moderate fusibility that can be remarkably enhanced by the addition of boron-bearing sludge.

## Acknowledgements

This study was carried out within the CNR-CONICET agreement (Project “Sustainable ceramic manufacturing: limits and improvements from dry milling and influence of the raw materials used”).

## REFERENCES

- [1] B. Karasu, Use of borax solid wastes in ceramics' world, in: Proc. 10th Intern. Conf. ECeS. Baden-Baden, Göller, 2008, pp. 1773–1778.
- [2] B.P. Tarasevich, G.D. Ashmarin, P.A. Ivashchenko, V.M. Gonyukh, O.S. Sirotkin, E.V. Kuznetsov, Polyborates as modifiers for nonvitrifying ceramic bodies, *Glass Ceram.* 40 (12) (1983) 604–607.
- [3] M. Özdemir, İ. Kıpçak, Recovery of boron from borax sludge of boron industry, *Miner. Eng.* 23 (9) (2010) 685–690.
- [4] R. Boncukcuoğlu, M.M. Kocakerim, E. Kocadağistan, M.T. Yılmaz, Recovery of boron of the sieve reject in the production of borax, *Resour. Conserv. Recycl.* 37 (2) (2003) 147–157.
- [5] C. Helvacı, F. Ortı, Zoning in the Kirka borate deposit, western Turkey: primary evaporitic fractionation or diagenetic modifications? *Can. Mineral.* 42 (4) (2004) 1179–1204.
- [6] C. Helvacı, Stratigraphy, mineralogy, and genesis of the Bigadiç borate deposits, Western Turkey, *Econ. Geol.* 90 (5) (1995) 1237–1260.
- [7] C. Helvacı, Mineral assemblages and formation of the Kestelek and Sultançayır borate deposits, in: Proc. 29th Int. Geol. Congr., Part A, 1994, pp. 245–284.
- [8] Y. Elbeyli, Y. Kalpaklı, J. Gülen, M. Piskin, M. Piskin, Utilization of borax waste as an additive in building brick production, in: Proceedings of the Uluslararası Bor Sempozyumu, Eskisehir, Turkey, 2004, pp. 23–25.
- [9] T. Uslu, A.I. Arol, Use of boron waste as an additive in red bricks, *Waste Manage. (Oxford)* 24 (2) (2004) 217–220.
- [10] T. Kavas, Use of boron waste as a fluxing agent in production of red mud brick, *Build. Environ.* 41 (12) (2006) 1779–1783.
- [11] G. Kaya, B. Karasu, E. Karacaoglu, Utilizing of borax solid wastes in roof tile and brick bodies, in: Sohn International Symposium, Advanced Processing of Metals and Materials, Volume 1: Thermo and Physicochemical Principles: Non-Ferrous High-Temperature Processing, 2006, pp. 535–543.
- [12] G. Kaya, B. Karasu, E. Karacaoglu, Effects of fritted borax solid wastes on the properties of brick bodies, *Silic. Ind.* (11–12) (2009) 363–367.
- [13] A. Christogerou, T. Kavas, Y. Pontikes, S. Koyas, Y. Tabak, G.N. Angelopoulos, Use of boron wastes in the production of heavy clay ceramics, *Ceram. Int.* 35 (1) (2009) 447–452.
- [14] A. Christogerou, T. Kavas, Y. Pontikes, C. Rathossi, G.N. Angelopoulos, Evolution of microstructure, mineralogy and properties during firing of clay-based ceramics with borates, *Ceram. Int.* 36 (2) (2010) 567–575.
- [15] M. Çolak, I. Ozkan, Sintering properties of the Bornova shale (Turkey) and its application in the production of red fired ceramics, *Ind. Ceram.* 31. (3) (2011).
- [16] A. Kilicarslan, Y. Kurttepelı, M.N. Sarıdede, Using of boron wastes in red brick production, *Adv. Mater. Res.* 699 (2013) 223–227.
- [17] N. Ediz, H. Yurdakul, A. Issi, Use of tincal waste as a replacement for calcite in wall tile production, *Key Eng. Mater.* 264 (2004) 2457–2460.
- [18] N. Ediz, A. Issi, H. Yurdakul, Effect of tincal waste addition to replace silica sand in wall tile production, *Key Eng. Mater.* 264 (2004) 2465–2468.
- [19] A. Olgun, Y. Erdogan, Y. Ayhan, B. Zeybek, Development of ceramic tiles from coal fly ash and tincal ore waste, *Ceram. Int.* 31 (1) (2005) 153–158.
- [20] S. Kurama, A. Kara, H. Kurama, The effect of boron waste in phase and microstructural development of a terracotta body during firing, *J. Eur. Ceram. Soc.* 26 (4) (2006) 755–760.
- [21] S. Kurama, A. Kara, H. Kurama, Investigation of borax waste behaviour in tile production, *J. Eur. Ceram. Soc.* 27 (2) (2007) 1715–1720.
- [22] İ. Özkan, Utilization of Bigadiç boron works waste clay in wall tile production, *Acta Phys. Pol. A* 132 (3) (2017) 427–429.
- [23] N. Ediz, A. Yurdakul, Characterization of porcelain tile bodies with colemanite waste added as a new sintering agent, *J. Ceram. Process Res.* 10 (4) (2009) 414–422.
- [24] N. Ediz, A. Yurdakul, Development of body formulations using colemanite waste in porcelain tile production, *J. Ceram. Process Res.* 10 (2009) 758–769.
- [25] H. Celik, Recycling of boron waste to develop ceramic wall tile in Turkey, *Trans. Indian Ceram. Soc.* 74 (2) (2015) 108–116.
- [26] B. Karasu, G. Kaya, R. Kozulu, Utilisation of concentrator wastes of Etibor Kirka Borax Company in the recipe of an opaque frit used for wall tile glazes as an acid boric replacement, *Key Eng. Mater.* 264 (2004) 2505–2508.
- [27] B. Karasu, G. Kaya, A. Cakir, S. Yesilay, Utilization of borax solid wastes in fast single-firing porcelain tile glass-ceramic glazes under industrial working conditions, in: REWAS'08, 2008, pp. 379–387.
- [28] K.K. Pekkan, B. Karasu, A. Kucuk, Production and industrial adaptation of fast single firing wall tile opaque glass-ceramic glazes containing borax solid wastes, in: REWAS'08, 2008, pp. 371–378.
- [29] K. Pekkan, B. Karasu, Evaluation of borax solid wastes in production of frits suitable for fast single-fired wall tile opaque glass-ceramic glazes, *Bull. Mater. Sci.* 33 (2) (2010) 135–144.
- [30] G. Kaya, B. Karasu, A. Cakir, Characterisation of diopside-based glass-ceramic porcelain tile glazes containing borax solid wastes, *J. Ceram. Process Res.* 12 (2) (2011) 135–139.
- [31] B. Cicek, A. Tucci, E. Bernardo, J. Will, A.R. Boccaccini, Development of glass-ceramics from boron containing waste and meat bone ash combinations with addition of waste glass, *Ceram. Int.* 40 (4) (2014) 6045–6051.

- [32] A. Moreno, J. Garcia-Ten, E. Bou, A. Gozalbo, J. Simon, S. Cook, M. Galindo, Using boron as an auxiliary flux in porcelain tile compositions, in: *Proceedings of the 6th World Congress on Ceramic Tile Quality—QUALICER 2000*, 2000, pp. 77–91.
- [33] S.M. De Paula, A. Albers, Effect of borates on the vitrification behaviour of a porcelain type tile body, in: *Proceed. 7th World Congress on Ceramic Tile Quality—QUALICER 2002*, vol. 3, 2002.
- [34] E. Yersel, B. Tufan, T. Batar, A study of various boron additives on the mechanical behaviour and microstructure of ceramic tiles, *J. Ore Dress.* 12. (24) (2010).
- [35] S.U. Bayca, T. Batar, E. Sayin, O. Solak, B. Kahraman, The influence of coal bottom ash and tincal (boron mineral) additions on the physical and microstructures of ceramic bodies, *J. Ceram. Process Res.* 9 (2) (2008) 118–122.
- [36] O.V. Kichkailo, I.A. Levitskii, Effect of colemanite additions on sintering, properties, and microstructure of spodumene heatproof ceramic, *Glass Ceram.* 68 (1–2) (2011) 56–60.
- [37] F.G. Melchiades, L.R. dos Santos, S. Nastro, A.O. Boschi, Gres porcelánico esmaltado producido por vía seca: materias primas fundentes, *Bol. Soc. Esp. Ceram. Vidr.* 51 (2) (2012) 133–138.
- [38] S.U. Bayca, Effects of the addition of ulexite to the sintering behavior of a ceramic body, *J. Ceram. Process Res.* 10 (2) (2009) 162–166.
- [39] S. Somany, G.G. Trivedi, T. Sridhar, A. Goel, D. Mohanty, B. Pitchumani, Increase in vitrified tile production by the use of borate flux, in: *Proceed. 13th World Congress on Ceramic Tile Quality—QUALICER 2014*, 2014.
- [40] A.F. Gualtieri, Development of low-firing b-fluxed stoneware tiles, *J. Am. Ceram. Soc.* 92 (11) (2009) 2571–2577.
- [41] S.B. Carpenter, R.B. Kistler, Boron and borates, in: J. Elzea Kogel, N. Triveldi, J.M. Barker, S.T. Krukowsky (Eds.), *Industrial Minerals and Rocks. 7 Th.*, SME, USA, 2006, pp. 275–285.
- [42] J.C. Turner, Estratigrafía del Nevado de Cachi y sector al oeste (Salta), *Acta Geol. Lilloana* 3 (1960) 191–226, Tucumán.
- [43] R.N. Alonso, Boratos terciarios de La Puna, Jujuy, Salta y Catamarca, in: E.O. Zappettini (Ed.), *Recursos Minerales de la Republica Argentina*, Anales, vol. 35, Instituto de Geología y Recursos Minerales SEGEMAR, Buenos Aires, 1999, pp. 1779–1826.
- [44] A.C. Larson, R.B. Von Dreele, *General Structure Analysis System (GSAS)*. Los Alamos National Laboratory Report No. LAUR 86-748, Los Alamos National Laboratory, New Mexico, USA, 1988.
- [45] H. Toby, EXPGUI, a graphical user interface for GSAS, *J. Appl. Crystallogr.* 34 (2001) 210–213.
- [46] A.F. Gualtieri, Accuracy of XRPD QPA using the combined Rietveld–RIR method, *J. Appl. Crystallogr.* 33 (2000) 267–278.
- [47] C. Zanelli, M. Raimondo, G. Guarini, M. Dondi, The vitreous phase of porcelain stoneware: composition, evolution during sintering and physical properties, *J. Non-Cryst. Solids* 357 (2011) 3251–3260.
- [48] S. Conte, C. Zanelli, M. Ardit, G. Cruciani, M. Dondi, Predicting viscosity and surface tension at high temperature of porcelain stoneware bodies: a methodological approach, *Materials* 11 (2475) (2018) 16.
- [49] T. Ban, K. Okada, Structure refinement of mullite by the Rietveld method and a new method for estimation of chemical composition, *J. Am. Ceram. Soc.* 75 (1992) 227–230.
- [50] D. Giordano, J.K. Russell, D.B. Dingwell, Viscosity of magmatic liquids: a model, *Earth Planet. Sci. Lett.* 271 (2008) 123–134.
- [51] A. Dietzel, Relation between the surface tension and the structure of molten glass, *Kolloid-Z.* 100 (1942) 368–380.
- [52] A.A. Appen, *Chemistry of Glass (Russ.)*, Khimiya, Leningrad, 1974, pp. 351.
- [53] M. Dondi, G. Guarini, I. Venturi, Assessing the fusibility of feldspathic fluxes for ceramic tiles by hot stage microscope, *Ind. Ceram.* 21 (2) (2001) 67–73.
- [54] M. Dondi, Feldspathic fluxes for ceramics: sources, production trends and technological value, *Resour. Conserv. Recycl.* 133 (2018) 191–205.
- [55] F. Contartesi, F.G. Melchiades, A.O. Boschi, Anticipated overfiring in porcelain tiles: effects of the firing cycle and green bulk density, *Bol. Soc. Esp. Ceram. Vidr.* (2018), <http://dx.doi.org/10.1016/j.bsecev.2018.07.001>.
- [56] D.B. Dingwell, R. Knoche, S.L. Webb, M. Pichavant, The effect of B<sub>2</sub>O<sub>3</sub> on the viscosity of haplogranitic liquids, *Am. Mineral.* 77 (1992) 457–461.
- [57] M.O. Prado, E.D. Zanotto, R. Müller, Model for sintering polydispersed glass particles, *J. Non-Cryst. Solids* 279 (2–3) (2001) 169–178.